“Screening toolkit for the assessment of fluid flow through fractures in shale”

Asif Hoq

Churchill College

TECHNICAL ABSTRACT

Hydraulic fracturing of shale is becoming increasingly popular with companies in the extraction of unconventional sources of gas. The basic process has been in action for the last sixty years but it has become controversial with the public only recently. There are several environmental concerns associated with the processes behind “fracking” and an important one is the fear that the harmful fracturing fluid might actually contaminate the useable groundwater resources. Some areas around existing fracturing wells in the US showed signs of such contamination. This problem has triggered new research, indefinite bans in some countries and development of better monitoring techniques. The fourth year research project was set up to address this problem in a particular way.

The primary objective of the project was to investigate the flow rates out of the artificial cracks created by hydraulic fracturing and comparing them to industry values. Part of the project was also to find out how far the fracturing fluid can travel in the direction of useable aquifers. This meant that a toolkit would have to be created to assess fluid flow around fractures.

The investigation was initiated by first choosing an appropriate modelling tool. After some careful screening, a FORTRAN based simulator – PHAST, was chosen as it had the capabilities of modelling multi-component groundwater flow, solute transport and geochemical reactions. The software was then used to design and simulate six conceptual vertical fracture models. This helped in comparing results to the initial hypothesis and making sure that the values were reasonable. The results that were produced indicated that very low volumes of water leaked out of the fractures for low porosity surroundings whereas the same volumes were significantly high when the surrounding porosities were increased by just 40%. Pore velocity outputs were also obtained from the simulations and the results helped understand how the values change across the different geological layers. The

conceptual models were also a means for justifying some assumptions and understanding the limitations of the software. The lessons learnt from the initial demonstration cases were then put to use during the simulation of the case study.

In this investigation, the Barnett shale play was chosen as the case study. This Texan field has seen extensive production over the last ten years. The next part of the project compared the Barnett data to the ones collected for all the other U.S. shale plays, in order to justify the choice of Barnett as the case study. The comparisons proved that the Barnett properties are closer to the average values than any other existing shale field, thereby making it a viable choice for a case study.

This was followed by the modelling of the Barnett with PHAST. The model was more complex than the previous scenarios and saw a few modifications. Average flow rates and the pore velocities, were once again the outputs that were calculated in the simulation. The results showed that the total estimates of the leaked water volumes were reasonable compared to industry values. The velocity results obtained were insignificant but these values were expected to be even lower if flowback pressure and geochemical reactions were to be considered in the model. PHAST has the capabilities of modelling these and many other features depending on the needs of the user. And hence, this tool can be adapted for other shale plays which would help in estimating flow out of the fractures.

As hydraulic fracturing processes impose potential environmental threats, it is important for engineers to be able to assess the risks before mitigating or preventing them using a combination of tools. And hopefully the outcome and the results of this research project will in a way add value to the existing industry toolkits.

Screening toolkit for the assessment of fluid flow through fractures in shale

by

Asif Hoq (CHU)

Fourth-year Undergraduate Project

in Group D, 2011/2012

"I hereby declare that, except where specifically indicated, the work submitted herein is my own original work."

Signed:

Date:

1. INTRODUCTION

The global demand for energy is expected to increase by 70 per cent by 2050 (Foda et al. 2011). Judging from current trends, most of this demand will be met by fossil fuels as countries are trying to make a smooth transition towards renewable sources of energy. Their interests are turning towards unconventional sources of fossil fuels as a short term compromise, such as tight gas present in shale rock. In order to exploit these hydrocarbon rich sources, hydraulic fracturing is used to create artificial cracks in the shale using very high pressured water. Over the past fifty years, hydraulic fracturing has helped deliver over 600 trillion cubic feet of natural gas to the world. And yet the current technologies are still very energy and water expensive with numerous environmental concerns – making it a controversial topic in many countries, especially in the UK and France.

A single hydraulic fracturing well can use millions of gallons of water – which contains a mix of hazardous chemicals to aid in the fracturing procedure. Studies have shown that 20-75% of the water is lost in the well depending on the site (U.S. Environmental Protection Agency 2010), which gives a cause for concern of aquifer contamination. This project was set up to investigate this problem by laying out the following objectives:

- Find ways to quantify the water leakage from fractures caused by “fracking”
- Investigate the rate of frac fluid approaching the shallowest aquifer in a conceptual model and compare these to industry predictions
- Gain a good understanding of the concepts, parameters and limitations involved in the modelling of fracture stimulation

A study evaluating the potential release scenarios from hydraulic fracturing was carried out focusing on a conceptual model of an environmental system and the possible concentrations of chemicals present in the fracturing fluid (U.S. EPA 2011). The paper acknowledges that the next stage of their investigation would be to include data from hydrogeology, geochemistry and chemical properties. Another relevant study was conducted on groundwater flow in fractured rock aquifers (Cook 2003). It shed light on how

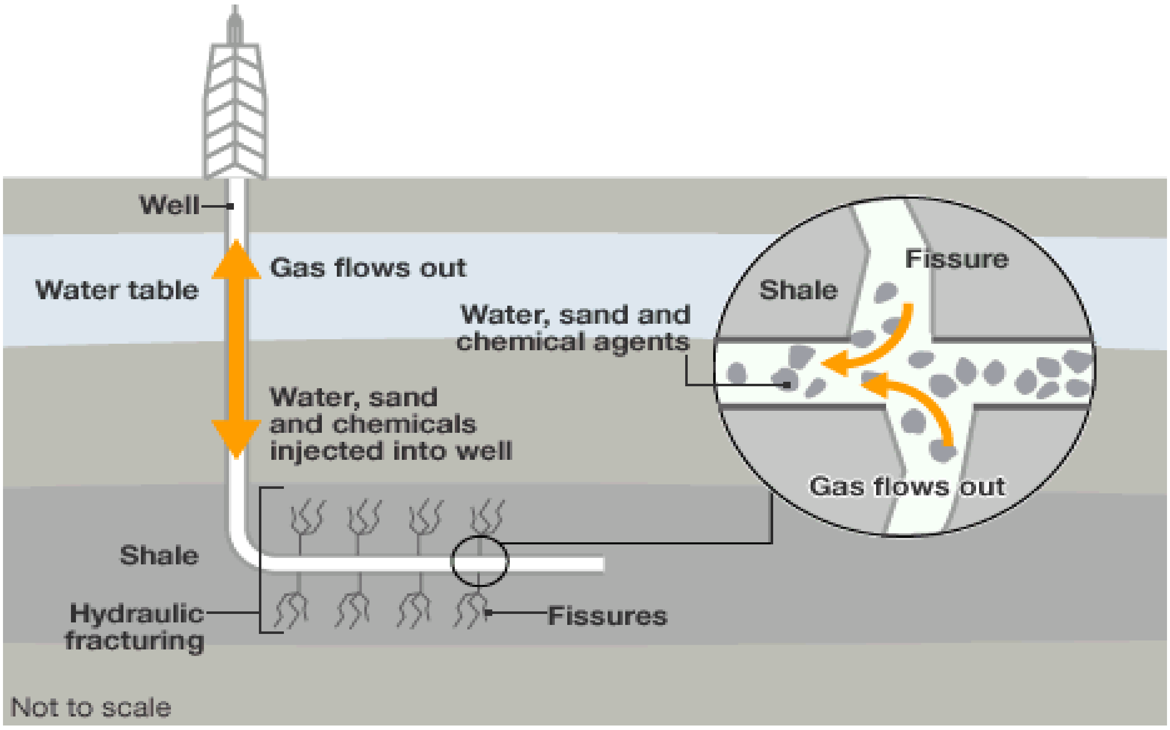

Figure 1.1 – Shale gas extraction. Note: The distance between the water table and the shale layer is heavily out of scale. They are usually about 1800 metres apart.*

**Courtesy of the BBC*

groundwater would behave around natural fractures but did not discuss anything about flows out of artificial fractures in deeper shale.

Hence, both of the two studies mentioned above were relevant to this project by some degree. This investigation was aimed at understanding flow from fractures in shale and estimating the chemical concentrations around them – thereby combining the purposes of the two aforementioned studies. Based on the initial knowledge and understanding of the subject, a hypothesis had to be established. The investigation was expected to show high volumes of water penetrating into the shale region but insignificantly small amounts escaping out of this layer. It was also predicted that the frac fluid would not be able to reach useable groundwater levels.

Hydraulic Fracturing and the Barnett shale

An appropriate amount of background knowledge was necessary before initiating the research. The process of hydraulic fracturing involves large volumes of fluid being pumped into shale layers which can be up to 2 km deep underground – equivalent to seven *Shard* skyscrapers on top of one another. Shale is a fine grained sedimentary rock and on average has porosities of about 3-5% (U.S. Energy Information Administration 2011) with really low hydraulic conductivities. It is often surrounded by other rock layers, such as limestone and sandstone. Due to the unique nature of shale, every single source is different and no assumption can be taken for granted (Halliburton 2008). The fracturing process is initiated by pressurizing the fluid to values of more than the fracture gradient of the geology. This creates a network of fractures within the shale giving every gas molecule a high speed path to the well bore. Next stage involves the fracturing fluid being pumped back to the surface pulling out the hydrocarbons in the process. This is known as the flowback fluid and there have been growing environmental concerns about its' safe disposal. Hydraulic fracturing fluids contain mixes of sand, resins and chemicals which help throughout the process. Hydraulic fracturing fluid additives are discussed in more detail in Appendix D. Hence, there have also been public concerns and fears as to if the fracturing fluids contaminate the shallow aquifers. Shale gas production has been very unpopular with the public in Europe where it has seen a nationwide ban in France and in Bulgaria. The UK has some shale reservoirs in the North, but its extraction has been put on hold until accurate risk assessment and evaluations of the hazards are established (Cox 2011).

The US on the other hand has seen extensive activity in shale gas production. This gave access to detailed information to the related geologies, fracturing techniques and production rates. Therefore it seemed appropriate to choose an existing US field as a case study for this research. The recent advances in horizontal drilling have made it possible to commercially access the Texan Barnett Shale and since the early 2000s this shale play has been presumed to have the largest recoverable resources than any other onshore US gas field (TPG 2011). The reasons for choosing the Barnett as a case study are justified later in this document.

2. METHODS

2.1 Software review

A suitable software was necessary to simulate the fracturing models in mind. The software would have to be able to model groundwater flow with capabilities for solute transport. Following some careful screening, the choice was narrowed down to three modelling tools.

PHAST – a FORTRAN based program combining best of the PHREEQC and HST3D packages, looked promising as the appropriate tool. It is capable of simulating multi component, reactive solute transport in three-dimensional saturated groundwater flow systems (U.S. Geological Survey 2010). Another advantage of PHAST is that the size of the grid cubes could be independently and easily adjusted, e.g. increasing the resolution of the grids where the fracture is placed. It was chosen over MODFLOW primarily due to its potential in simulating reactive solute transport. MODFLOW is a great ground water modelling tool but requires separate software – 3DST, to process the primary outputs if chemical transport results are desired. PHREEQC also stood out as a program written in the C programming language for modelling geochemical reactions and diffusion. But it wasn't as versatile as PHAST with regards to groundwater flow.

The inputs required for PHAST modelling are comprised of three separate text files. The first one is a trans.dat file for the flow and transport data calculations. This file can be produced with the help of the graphical user interface. The chem.dat text file consists of the chemical reaction calculation data which can only be modified manually. And the third file is phast.dat – a thermodynamic and chemical database file which is necessary if chemical reactions are being modelled.

	Groundwater flow	Chemical transport	Open source
MODFLOW	✔		✔
PHREEQC		✔	✔
PHAST	✔	✔	✔

Figure 2.1 – Comparisons between the three software packages most relevant to the aims of the project

A separate graphical user interface called ModelMuse was used to model cases in PHAST and MODFLOW. This was perfect for modelling the conceptual cases as it simplified the complex PHAST code and offered a wide range of tools by being compatible with MODFLOW. Therefore if at any point the functions offered by PHAST were to be insufficient for modelling the cases, then MODFLOW could be used given that it was the second best choice for the task at hand.

2.2 Conceptual model methods

The next stage of the investigation was to model a series of fracture scenarios differentiated by the fracture length, position and the geologies involved. The initial six proposed cases – illustrated in Figure 2.2, were not based on any existing shale plays, but were made up based on the general geological information of shale rock (U.S. Energy Information Administration 2011). The underlying question was simple – "What happens if the fracture propagates through layers with distinct variations in porosity?" This is not in any way implying that current hydraulic fracturing practices are inefficient and lack accuracy. In fact the shale fracturing techniques at present are very well engineered and utilize sophisticated

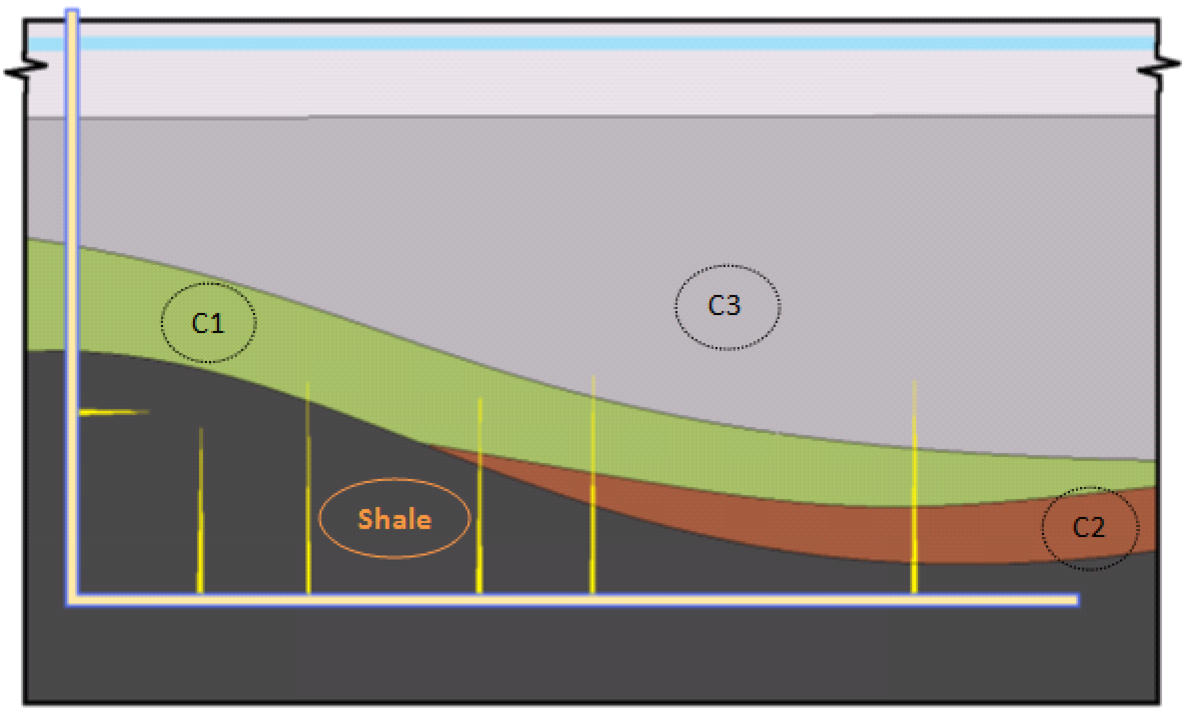

Figure 2.2 – Overall conceptual model of the geology around the shale. Each fracture represents a case to be simulated using PHAST. [C1 – Sandstone, C2 – Clay, C3 – Limestone]

monitoring methods.

The purpose of the demonstration runs was to compare the flow rates associated with different properties. These cases were also expected to help in understanding the capabilities and limitations of the modelling software – which is discussed later. In reality, fracture geometry can be complex consisting of networks of smaller fractures. But for the sake of this investigation they were modelled as thin straight line cracks. The shale layer is blanketed by layers of sandstone (C1), clay (C2) and limestone (C3). These assumptions are theoretical and can later be adjusted if necessary during the simulations. In reality, 1 metre long fracture is very unlikely to penetrate through four different layers as shown in figure 2.2. The proposal of different layers is an extreme substitute for varying porosities within the shale. Out of the initial six fracture models displayed, five have been modelled around a horizontal well. The flows that would be investigated from these different scenarios would help understand how important the properties of the soil are to the "frac" fluid seepage. *Case 1* is the basic scenario where only a simple fracture is considered in the shale region. Whereas *case 4* is the most complicated one, as the fracture penetrates through four different layers.

In *Case 1* the fracture only penetrates the shale layer and the geology surrounding it was considered to be sandstone. The aim of the run was to see how much of the fracturing fluid escapes into the shale layer under extreme boundary conditions. And therefore, at this stage the properties of the layer surrounding the shale are not of much importance. Hence, sandstone was the primary assumption. The porosity of shale rock ranges between 0.5 - 8% - and hence, it is expected that a small amount of fracturing fluid would diffuse out of the fracture.

In *case 2*, the fracture propagates through the shale and the sandstone layer. The properties of shale are significantly different from the properties of sandstone (Appendix A), and this would almost certainly affect the fracture geometry. The network of fractures would cover a much larger radius in the sandstone layer due to its' lower fracture gradient, resulting in more fluid dispersion. Throughout this investigation the fracture geometry is assumed to be unaffected by the geologies and considered as a straight crack.

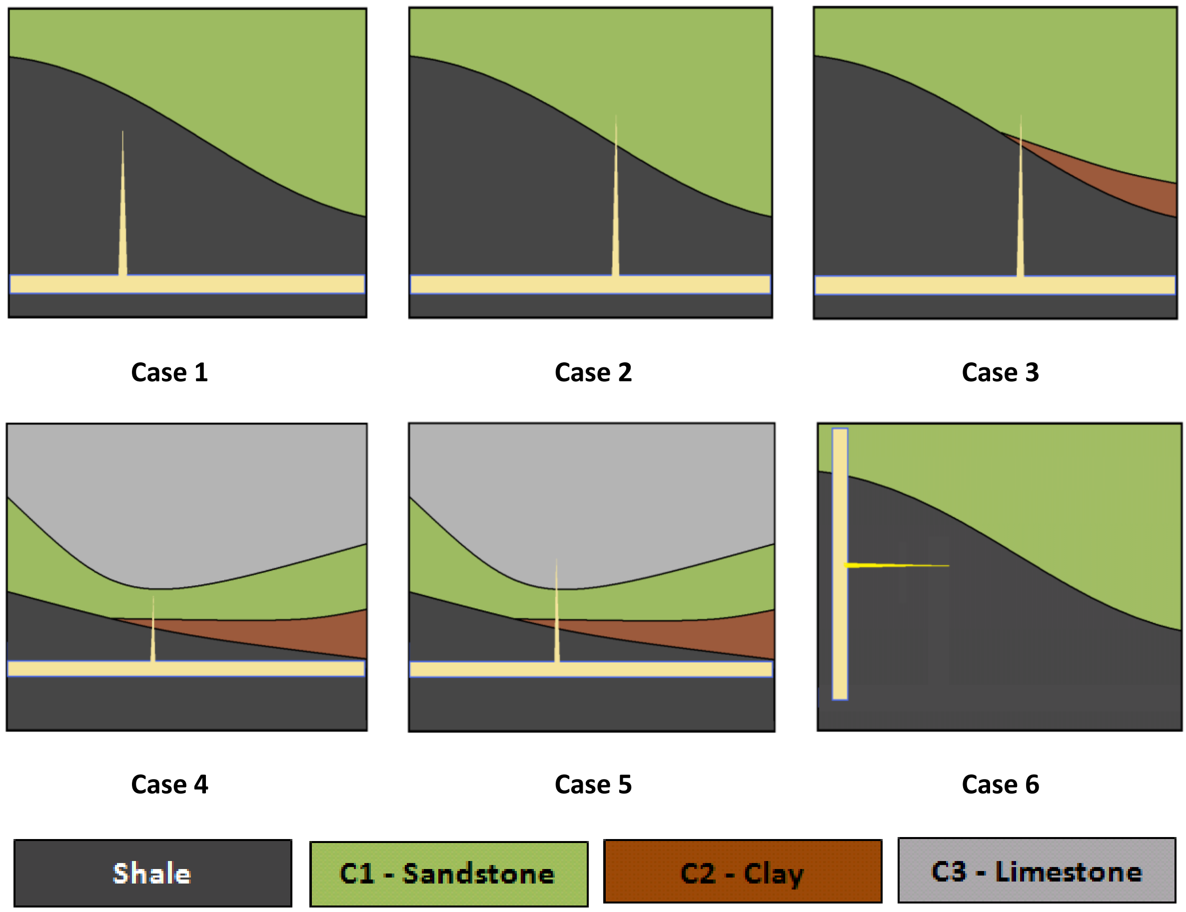

Figure 2.3 – Diagrams of the individual cases displaying the positions of the fractures with respect to the surrounding shale layer

Cases 3 and *4* see the fracture penetrating through three and four layers respectively. In these two cases, most of the fracture is exposed to geologies other than shale. This would undoubtedly increase the average flow rate of fracturing fluid from these fractures.

Case 5 is an extreme scenario where fluid diffusion will occur predominantly in the clay and limestone layers. As illustrated in Figure 2.3, *case 6* is a horizontal fracture from a vertical well. In practice, vertical wells are rarely used nowadays and are never used in conjunction with horizontal wells. This fracture model was optional and was considered in case the further investigations were required.

2.3 PHAST Parameters

The contents of the transport.dat file can be modelled with the help of ModelMuse. The first inputs that are required are the grid dimensions. For the demonstration runs, the model block had an area of 1km^2 with a depth of 200 metres. The characteristics for this grid matrix can be set through the data set function which demands a number of property values, such as porosity, hydraulic conductivities, specific storage, dispersivities and the initial heads. For instance, in *Case 1*, the grid matrix had the properties of shale. The limestone layer was modelled as an additional object with different values for the same property criteria. Once the geology had been set up, the fractures could then be modelled. For all of the DEMO runs, the fracture was modelled as a line with a specified initial hydraulic head. The head can also be varied with time if it is required for the investigation. In the case of the DEMO runs, the hydraulic head was set to zero after the first time step. In other words, if the time step is an hour long, then the hydraulic head will only be at the specified value for the first hour and zero in the following time steps. The hydraulic head is determined by estimating the fracture gradient of the shale rock in consideration. The average pressure gradient of shale is about 0.52psi/ft (=11.76Kpa/m) and can go up to 1.17psi/ft (LaFollette 2010). Multiplying these values with the average depth of shale formations gives the fracture gradient – the minimum pressure required to fracture the rock. These were calculated to be around 2400m and 6000m for an average and an extreme pressure gradient respectively. In the case of the DEMO runs, simulations were carried out using both head values. Along with the head, PHAST also demands the solution number, which is located in the chem.dat file. The same chemistry file was used for all of the simulations in this investigation for the sake of consistency. The constituents of the fracturing fluid were kept simple, albeit in practice it is a cocktail of complex compounds. In order to understand the chem.dat file, it was important to go back and understand PHREEQC. The chemistry files can be adapted to suit a diverse range of needs - from simple two element solutions to multi-component mixes with different charges, pH and densities. Sodium (Na) and chlorine (Cl) were the two chemicals considered in this investigation, both with densities of 10 moles per kg of water. This value in no way reflects the properties of real fracturing fluids, and is merely an assumption. It would be useful to consider a chloride in the solution as they are commonly used as tracers for groundwater flow. But since this investigation is limited to estimating the flow rates out of the fractures, chlorine seemed more relevant as it is a very reactive element and could provide some interesting results.

As expected, compromises and assumptions had to be made during the modelling process. First of all, it was difficult to model the geologies exactly as they were initially drawn, but it is hard to believe that this would have affected the results significantly. It was previously mentioned that hydraulic fracturing usually forms a complex network of small and larger fractures. In the DEMO cases, it was assumed that fracture would be a single three metre line. Fracture dimensions vary in the industry, but average lengths of 1m are common for the main stem (Daneshy 2010). Typically, fractures are branching structures – almost in a shape of a tree, rather than a single aperture. It was desirable for the model to have the same amount of surface area as in 'real life', so the fractures were designed as a single crack three metres long. The difference between one crack and several branching cracks should not affect the simulation results – this theory was tested and is explained in a few lines. Studies have shown how the presence of composite network of fractures allows the well to reach out deeper into the shale region, thereby increasing the productivity of a well (Daneshy 2010). For all of the models simulated in this investigation, the fracture was assumed to be a straight three metre line. To justify this assumption, a preliminary test was used to compare the flow rates between a branched and a straight fracture. The test was based on the geology of *case 1* with a fracture gradient of 6000m held for a day. The total surface area of fractures in contact with the shale was kept constant, i.e the sum of the lengths of the cracks in the branched scenario were approximately three metres. Also, the average flow rates were calculated at the grid where the fracture was placed in the model.

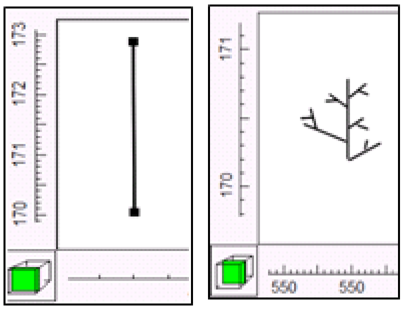

	Line (kg/s)	Branched (kg/s)
2days	1.18E-11	4.03E-10
4days	-5.39E-20	-4.83E-20

Figure 2.4 – Images of the two fracture scenarios (above) and their corresponding results (below)

The results from the test (Figure 2.4) showed that the branched fracture had a slightly higher flow rate than the line counterpart over the first time step. Despite the difference, the values are still comparable as they are both insignificantly small. For the second time step – three days after releasing the pressure, the two values were very similar with only a 10% difference between the results. This observation supports the assumption of a straight fracture for the models over medium to long periods of time. The critical factor was to equate the surface areas, which the model had done. Negative values for the flow rates are discussed later with the results of *Case 3*.

In the initial drawings of the concepts, the fractures were seen to be connected to the horizontal well. It was decided not to model the wells since they would not be contributing to the leakage at all. Nowadays the wells are finely cased all the way down to the shale formation with additional casing when it passes through useable groundwater levels. The casings are only broken at the points where hydraulic fracturing takes place and therefore only considering the leakage from the fracture is enough for this analysis.

Once everything relevant has been modelled, the output options had to be set up. PHAST allows the user to specify the output files of interest along with the respective print frequencies. In the case of the DEMO runs the print frequencies were set to two time units. This means that the program will calculate results every two time units once executed. For each case, four different simulations were conducted. First one was for an average pressure gradient of 2400m over 1 hour. This meant that the fracture would remain at the specified head for the first hour. The next three simulations were for extreme pressure gradients of 6000m over a minute, an hour and a day. In practice, wells are not kept at such high pressures for 24 hours. This was simulated out of curiosity to see what would happen with extreme pressures over a surreal time period. A pressure gradient of 6000 metres is a maximum value, which suggests that this would result in maximum flow rates.

3. DEMO RESULTS

Case 1

This was the first and the simplest model that was simulated. Illustrations on the right show the position of the fracture with the respect to the geological boundaries. The average flow rates achieved are also tabulated on the right. The results show that the amount of fracturing fluid that leaks out of the fracture is around 10^{-11}kg/s. The average flow rates of the fluid seem to stay constant. This means that the seepage rate into the shale stays constant irrespective of how long the fluid in the fracture stays under pressure. But the chlorine flow rates seem to propose something different. The average flow rates of chlorine decreases with longer pressured periods. This is most likely due to the fact that chlorine reacts with the constituents of the shale and hence the average flow (in and out of the fracture over two time units) is lowered since there is less of it with time. The bar graph on the right represents the chlorine mass flow rate on a log scale in the reverse order. From the plot, it is clearly visible that the Cl flow rate at 2400m is the same as when the fracture is at 6000m (both held for an hour).

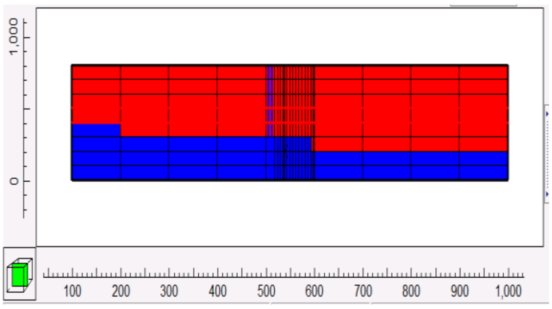

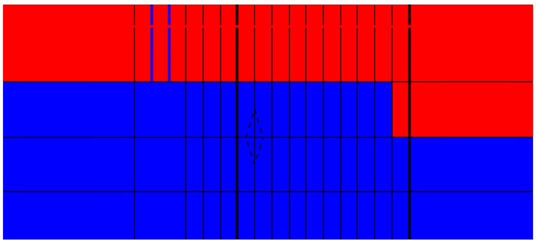

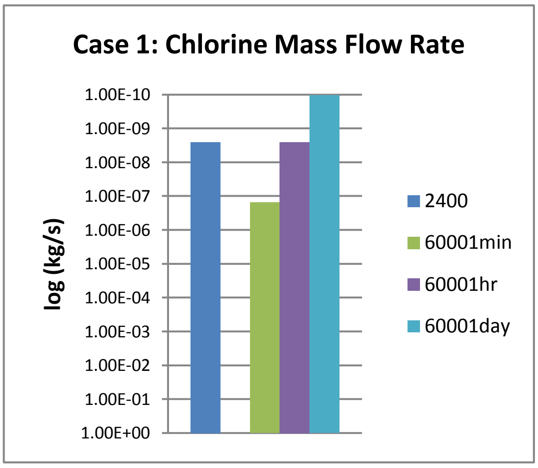

	Flow	Cl Flow
2400m – 1hr	4.72E-12	2.53E-9
6000m – 1min	1.18E-11	1.52E-7
6000m – 1hr	1.18E-11	2.53E-9
6000m – 1day	1.18E-11	1.06E-10

Figure 3.1 – Case 1 results. Views of the models in PHAST (top), bar graph of the chlorine mass flow rates over the four simulated scenarios (middle – n.b the Y-axis is set to the log scale and in the reverse order) and values of the average mass flow rates in kg/s from the simulations (bottom)

Case 2

In this case the fracture is modelled to penetrate through shale and sandstone. Since there are only two layers with different properties, the colour gradient consists of only two colours. Although the porosity of sandstone on average is almost 75% higher than that of limestone, they both have almost identical specific storage values. Similar to *case 1*, the results imply that the leakage rate does not depend on how long the fracture is under pressure. The chlorine flow also follows the pattern noticed in *case 1*. The average flow rates of the chemical decreases with longer pressured periods. It was expected that the flow rates would increase if the fracture were to penetrate through two or more layers. This is reflected in the table on the right. Leakage through sandstone and shale is increased by 377% compared to the results in *Case 1*, but they can still be considered as insignificant.

It is important to note that all these average flow rate values are calculated at the nearest node to the fracture.

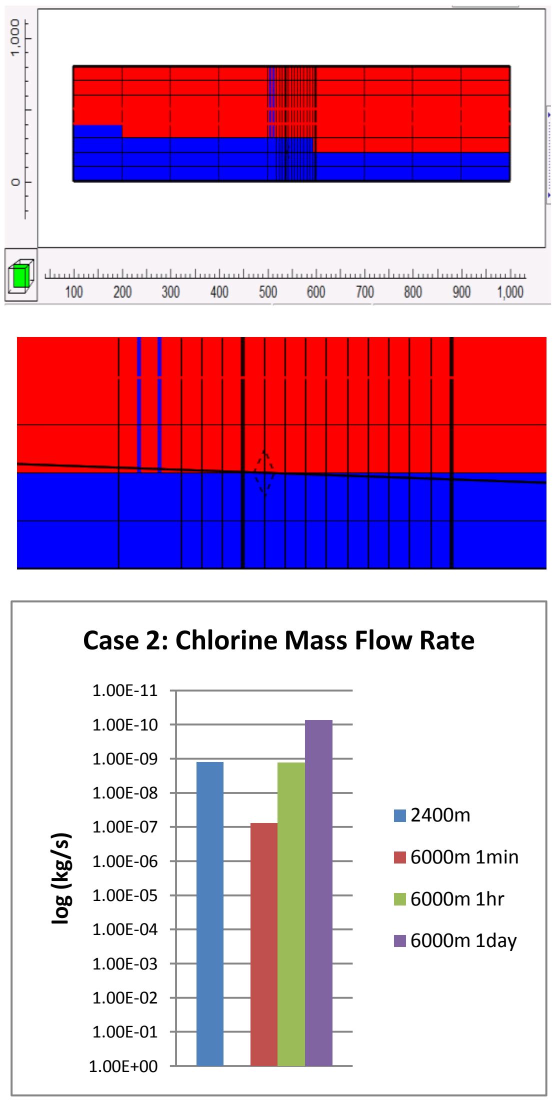

	Flow	Cl Flow
2400m – 1hr	2.25E-11	1.27E-9
6000m – 1min	5.63E-11	7.6E-8
6000m – 1hr	5.63E-11	1.29E-9
6000m – 1day	5.63E-11	7.28E-11

Figure 3.2 – Case 2 results. Views of the models in PHAST (top), bar graph of the chlorine mass flow rates over the four simulated scenarios (middle) and values of the average mass flow rates in kg/s from the simulations (bottom)

Case 3

In this scenario the fracture passes through three geological layers namely shale, clay and sandstone. Compared to its sedimentary counter parts, clay has much higher specific storage and a porosity of about 40%. Hence, it was expected that there would be significantly higher flow rates. The results produced were mostly negative. This unexpected result suggested that over the course of the two time periods the flow rates back into the fracture were much higher than the flow rates into the shale. The tabulated results display average flow rates over two time steps – since that was the default output frequency for all the runs. But for the second time step the pressure is set to zero. This would result in flow back into the fracture. This occurred in the previous two cases as well, but the flow rates back into the fracture weren't as high – probably due to the much smaller volumes of leakage. The average fluid flow rates are not constant anymore. This can be justified by the non-uniform layout of properties around the fracture.

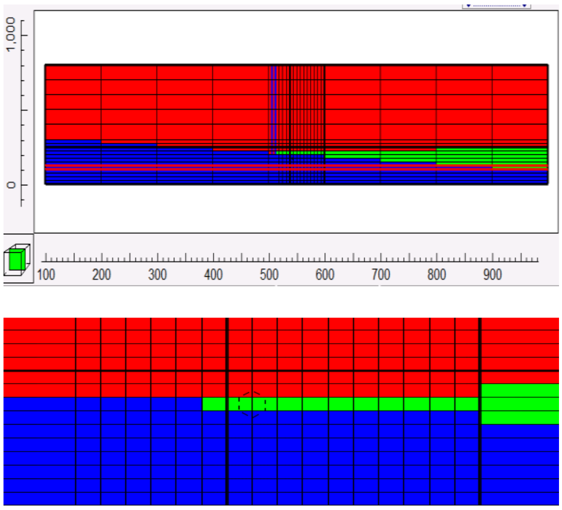

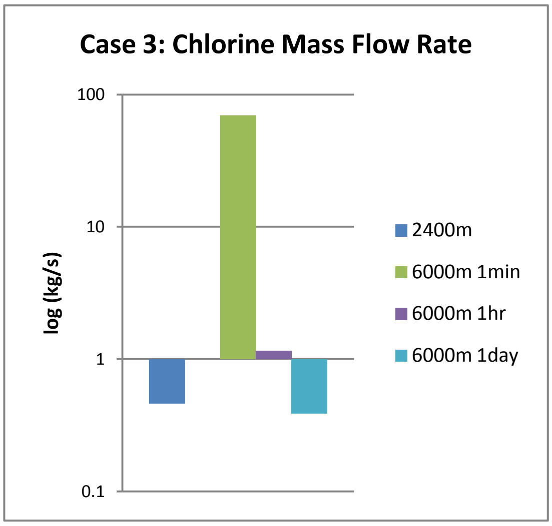

	Flow	Cl Flow
2400m – 1hr	-1.302	-0.462
6000m – 1min	-195.3	-69.25
6000m – 1hr	3.26	-1.15
6000m – 1day	-1.10	-0.389

Figure 3.3 – Case 3 results. Views of the models in PHAST (top), bar graph of the chlorine mass flow rates over the four simulated scenarios (middle) and values of the average mass flow rates in kg/s from the simulations (bottom – n.b negative values signify that there have been higher flow rates into the fracture rather than out)

Case 4

In this case the fracture propagates through four geological layers namely shale, sandstone, clay (green) and limestone (yellow). As illustrated, about 80% of the fracture is located outside the shale formation. Hence, higher flow rates were expected with negative values as obtained in *case 3*.

The results were similar to case three but all the values seemed to be scaled up by a factor of two. On average, *case 4* results hint that the flows back into the fracture were much higher than any of the other cases so far. They indirectly imply that the fracturing fluid that leaked out of the fracture in the first time period must have been significantly larger than the results from *case 1*.

So far the chlorine flow rate decreasing pattern has been consistent with all the four cases. This reinforces the theory signifying that chlorine ends up reacting with the surrounding geologies thereby gradually reducing from its initial amount.

It is important to note that results for all these cases are available up to 20 time steps. But the first time step is the most interesting one and therefore is the one that is always being considered.

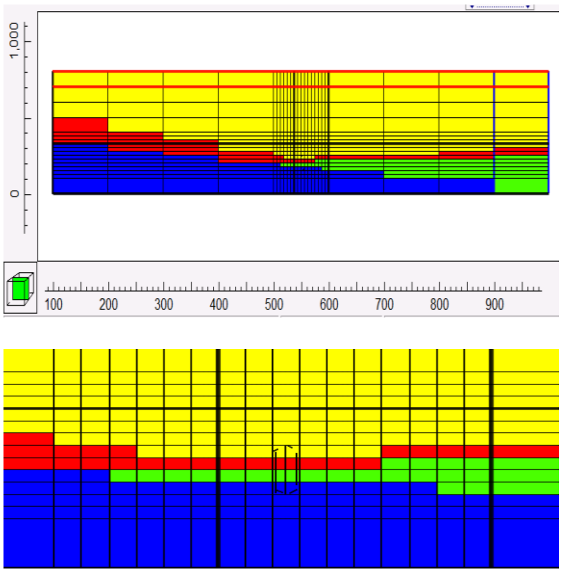

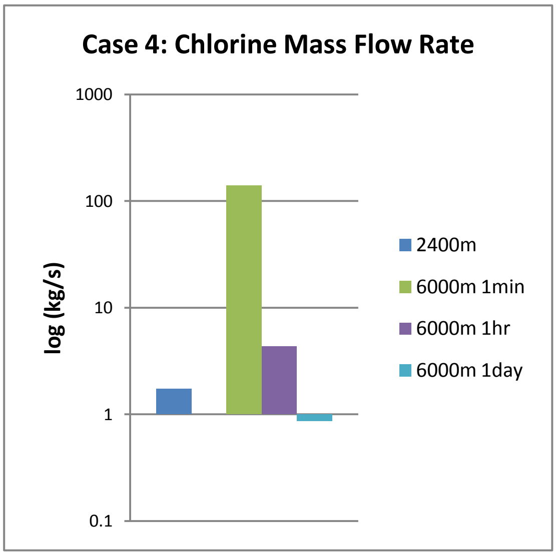

	Flow	Cl Flow
2400m – 1hr	-4.88	-1.73
6000m – 1min	-392.3	-139.12
6000m – 1hr	-12.21	-4.33
6000m – 1day	-2.45	-0.87

Figure 3.4 – Case 4 results. Views of the models in PHAST (top), bar graph of the chlorine mass flow rates over the four simulated scenarios (middle) and values of the average mass flow rates in kg/s from the simulations (bottom)

Case 5

This case is very similar to *case 4* with only a slight modification to the geology layout. This way the fracture is practically out of the shale region. And as a result, very high flow rates are again expected.

After the first time step (still two units of time), all the average flow results were negative. When the fracture is pressurised at 6000m for a minute, the resulting flow rate values are colossal. The average fluid flow rate is -39258kg/s – which would almost certainly rip through the small fracture networks. Obviously this value is impractical even for an overestimate, as it seems to resemble a large point source rather than a thin fracture. The reason why flow rates are highest during one minute pressurised periods is straightforward. There is not enough time to average out the flow rates compared to the other two situations where the flow rates are averaged over 3600 and 86400 seconds respectively.

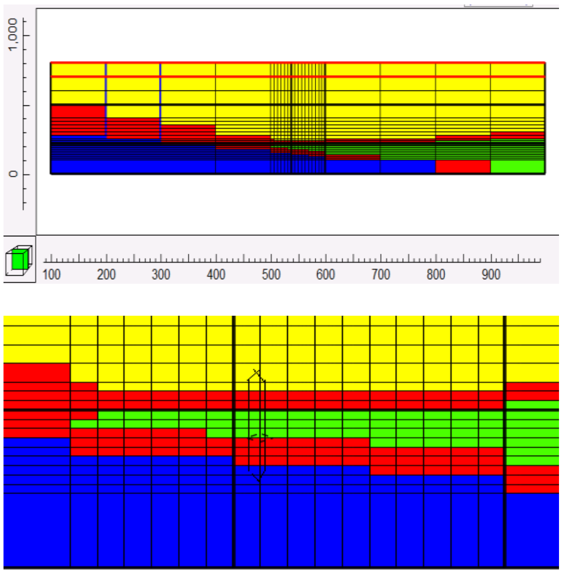

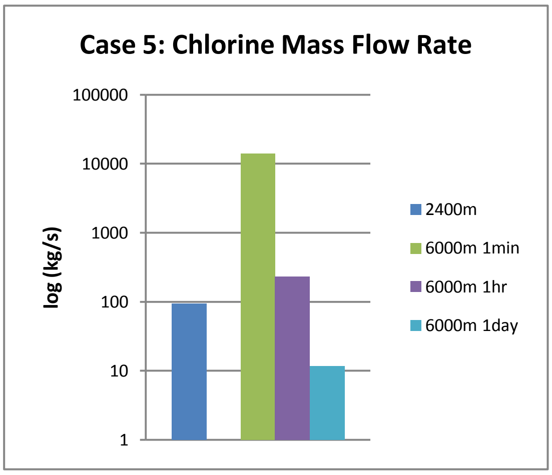

	Flow	Cl Flow
2400m – 1hr	-262.19	-92.94
6000m – 1min	-39258	-13918
6000m – 1hr	-655.47	-232.38
6000m – 1day	-33.04	-11.71

Figure 3.5 – Case 5 results. Views of the models in PHAST (top), bar graph of the chlorine mass flow rates over the four simulated scenarios (middle) and values of the average mass flow rates in kg/s from the simulations (bottom)

Case 6

This was the only scenario where a horizontal fracture was modelled considering vertical hydraulic fracturing wells. The results from this model were expected to be very similar to *Case 1* since fractures in both cases are only surrounded by shale. But the results achieved were on average a factor of 10^4 higher than the results achieved from *case 1*. This could be due to the fact that this time the fracture was modelled within one grid and did not cross any grid boundaries. In the previous five cases the fracture crossed a grid boundary at 170m even though most of it lay above this level. Despite the large percentage difference, the scale of the flow rate values is still comparable to the first two cases.

Also, the chlorine mass flow rate over the different pressured time steps exhibited a pattern similar to the first two cases. Comparing *cases 1, 2 and 6* suggests that the chlorine flow rates do not significantly depend on the fluid pressure when only shale is considered. In the three cases, the level of the flow rate of chlorine at 2400m is close to the level for 6000m over the same time unit.

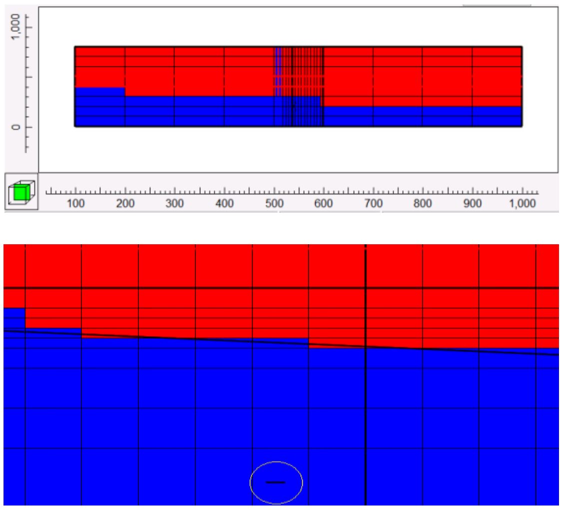

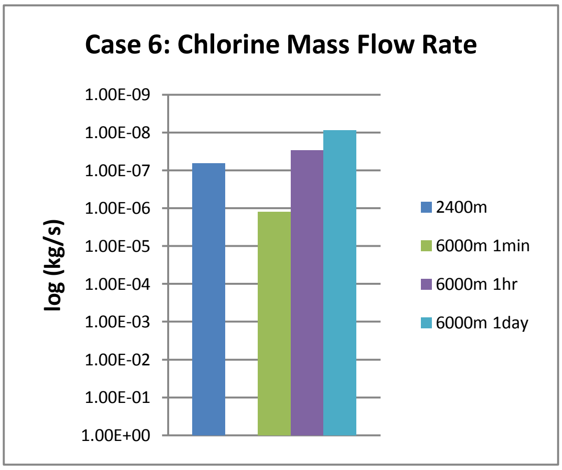

	Flow	**Cl Flow**
2400m – 1hr	1.25E-7	6.56E-8
6000m – 1min	2.23E-8	1.24E-6
6000m – 1hr	2.24E-8	2.94E-8
6000m – 1day	2.23E-8	8.83E-9

Figure 3.6 – Case 6 results. Views of the models in PHAST (top), bar graph of the chlorine mass flow rates over the four simulated scenarios (middle) and values of the average mass flow rates in kg/s from the simulations (bottom) Note the differences in scale in the outputs compared to cases 3, 4 and 5.

4. DEMO DISCUSSION

Not only did these six DEMO runs help to familiarize with PHAST but its results were essential in understanding the nature of the fluid flow rates. The scale of the results was reasonable and expected in the case of the first two scenarios. The decreasing pattern of chlorine flow was also justifiable. In order to quantify the mass of the fluid required per fracture, a time period must be chosen to be keeping it at one of the two pressures. For this particular investigation to work, it is also important to take the absolute values of the flow rates. Therefore, for the hour slot, the respective volumes of water and the comparisons between them are illustrated in Figure 4.1.

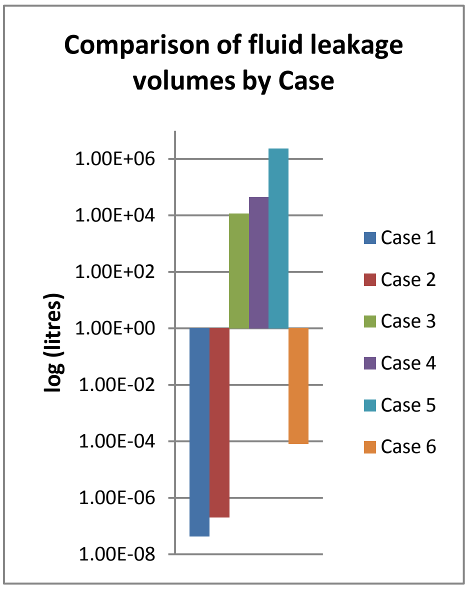

	Mass(kg)
Case 1	4.24E-8
Case 2	2.03E-7
Case 3	1.17E4
Case 4	4.4E4
Case 5	2.36E6
Case 6	8.06E-5

Figure 4.1 (a) and (b) – Comparison of the estimated volumes leaking out of the fracture between the six scenarios (a) and the values of these volumes tabulated in kg – demonstrating the large differences in scale (b)

The bar graph on the left clearly displays the vast scale differences of leakage volumes between the six cases. For *cases 1, 2 and 6* – the model calculates that the volume of fluid escaping from a single fracture is well below 0.0001 litres. On the other hand, results from *cases 3, 4 and 5* shows that these volumes can be up to 100,000 litres per fracture. For the worst case scenario – case 5, one fracture uses about 2,360,000 litres or 623,446 US gallons of fluid per hour. To put this into perspective – hydraulic fracturing of high permeability reservoirs can use as much as 2-3 million US gallons per well. The result from case 5 is about 30% of that value for one single fracture. Of course, this would never happen in a real life scenario since such high flow rates are inexistent. On the other hand, a 4.24E-8 litre per fracture is a very small number. Even after considering multiple fractures per well with multiple tries, the number doesn't even add up to one US gallon. But it is known that typical wells can consume from 80,000 to 1 million US gallons of fluid (Arthur et al. 2008). These values can be achieved only when the water in the rest of the well is considered. For instance, a well length of 1mile with a radius of 5m gives a volume of 125600m^3 equivalent to about 3,3180,009 US gallons - much closer to the practical values.

Average flow rates aside, PHAST can calculate many other results such as hydraulic heads, pore velocities, chemical concentrations and pH. The pore velocity output file consists of the velocities between consecutive grid blocks in the model. An analysis was carried using some of these results in order to compare and evaluate velocities from two different cases. Figure 4.2(b) represents a section of the X-Y plane on which the fracture is located. The fracture for all of the DEMO scenarios stretches between layers 2 and 3. For the analysis, the grids right above the fracture were taken into consideration – as shown on the diagram. This meant that the velocity values had to be sorted from all the others for a distinct grid location between every layer. The analysis compared these vertical velocities for *cases 3 and 4* – since these two produced reasonably high average flow rates which in theory would result in quantifiable velocity values. Figure 4.2(a) is a plot of the pore velocities against the time steps between two crossovers: 3-4 and 8-9. The former being the one encompassing the fracture and the latter being the top layer in the models. This set up was expected to show

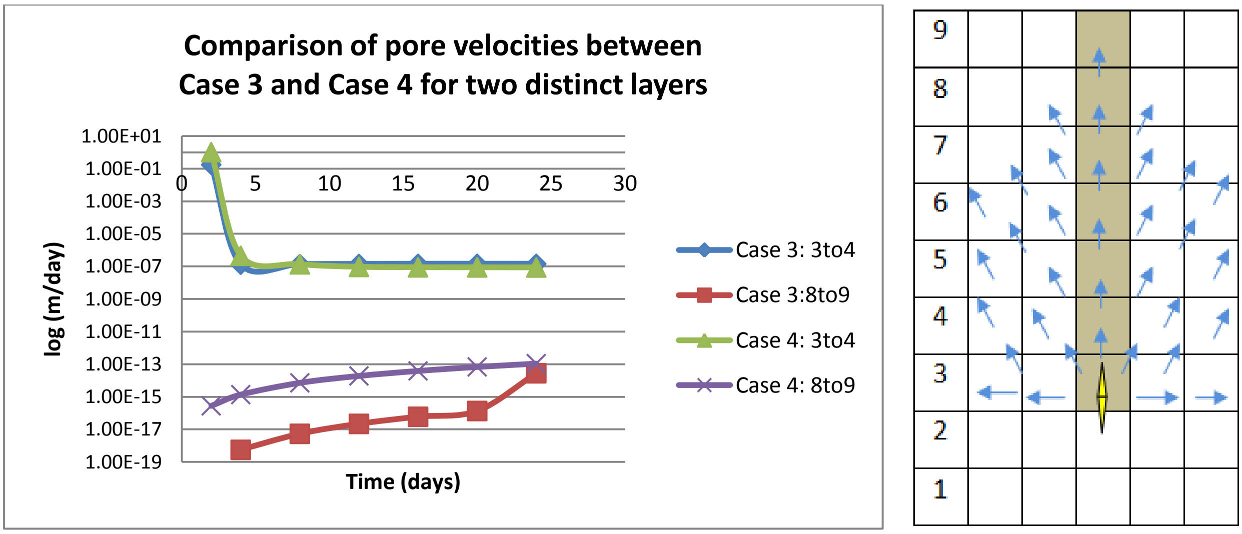

Figure 4.2 (a) and (b) - Plots of the change of pore velocities over time and across two specific layers – 3 to 4 & 8 to 9 (a). Diagram showing the expected fluid flow from the fracture across the layers 3 to 9 and the chosen vertical grids over which were considered for the pore velocity analysis (b).

the differences in velocities between the two extremes. The plot shows how the velocities between layers 3 and 4 over the calculated time steps (0 to 24 days) are very similar – with the values being in the same scale with a maximum of 40% difference between them. Over the first two time steps the pore velocity drops from about 1m/day to 10^{-7}m/day in both cases – decreasing with inverse proportions to the square root of time. With time, the velocity appears to approach a constant value. When the equivalent porous media conditions are reached, the distance travelled by the fluid will increase directly with time (constant velocity), as in the case for porous media aquifers. The shape of the plot corresponds to the change in solute velocity in fractured rock published in another study (Cook 2003). Comparing the velocities between layers 8 and 9, showed how *case 4* had higher velocities in general compared to case 3. This is very likely because the fracture was exposed to more non-shale geologies in the former scenario. But in both cases the values seemed to increase exponentially with time (n.b the Y-axis of the plot is in log scale). Calculating velocities over longer time steps should show these values approaching a constant value – similar to the previous two plots.

PHAST Capabilities

There are a few other ways a fracture could be modelled on PHAST. First one involves modelling a drawn line as a LEAKY boundary - under the PHAST boundary conditions function. This allows the user to specify the permeability of the surface area of the fracture and involves a few other adjustments to the inputs. A fracture could also be perhaps modelled as a reverse well. Instead of pumping out, a modified well could be told to pump in to the shale formation. This also involves restructuring of inputs and requires the pumping rate to be known. One could sit down and draw an intricate network of fractures as lines with specific heads, similar to the approach taken in this investigation. The consideration of a complex network will be a more realistic perception of the fractures even though the values do not differ that much (as seen previously). The PHREEQC chemistry file can be adapted to suit the needs of most users. To make this file more relevant towards hydraulic fracturing fluids, one could change the densities of the chemicals involved with respect to water – discussed later with more detail.

5. BARNETT STUDY METHODS

The Barnett shale first grabbed some real attention of engineers about 10 years ago, and extensive work has been done on it since then. As a result there are a lot of credible and relevant papers issued about this shale region, which makes it a good option for a case study (Waters et al. 2009; Fisher et al. 2004). The locations of all the US shale plays relative to the Barnett are illustrated on the map in figure 5.1(a).

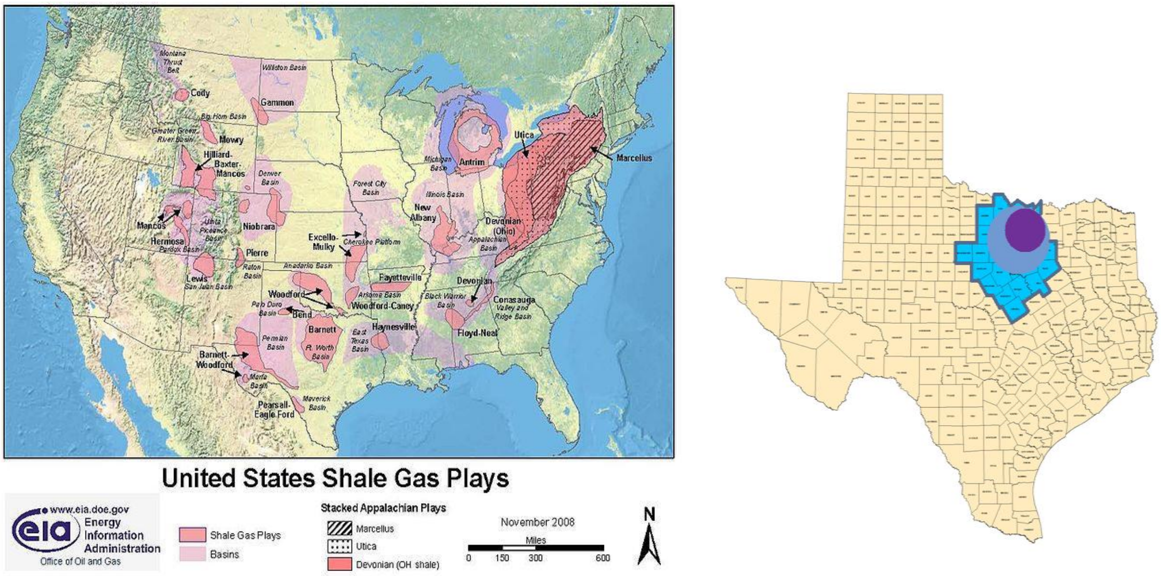

Figure 5.1(a) and (b) - Map of the US with the locations of the shale gas plays (a). Location of the core and the non-core areas within the Barnett shale play on a map of Texas (b).*

**Courtesy of the U.S. Energy Information Administration*

It is part of the Bend Arch-Fort Worth Basin – major petroleum producing geological system in the North of Texas. Figure 5.1(b) shows the outline of the Fort Worth Basin and the position of the shale plays within it depicted by two concentric circles. The smaller circle represents the "core" area where the shale is thicker and therefore reduces uncertainty. So far production has been focused in this part of the shale play. The larger circle shows the extent of the Barnett field productive area within the basin.

It was also the first shale field in the US on which horizontal drills were used commercially, hence corresponding with the scenarios that have been modelled on PHAST in this investigation.

Excluding the vastly unexplored Marcellus shale in the north-east, the Barnett formation contains about 10% of the shale gas reserves in the US. The US holds 13% of the world reserves. This means that the Barnett shale contains 1.3% of the worlds' technically recoverable shale resources. The next section shows comparisons of the Barnett shale with other significant formations in the US.

5.1 Comparison to other Shale plays in the US

Data was collected for 18 different shale formations across the US (U.S. Energy Information Administration 2011). This consisted of information on Estimated Ultimate Recovery (EUR), Technically Recoverable Resources (TRR), Porosity, Depth, Well Spacing, Thickness and the Total Organic Carbon Content (TOC). In order to compare these criteria with each other, their respective means and standard deviations were calculated. And using these values, normal distributions were created in the form of Bell Curves (Appendix B). But in order to compare Barnett to all these shale formations along with the different criteria, a better means of visualizing them had to be prepared.

The plots on figure 5.2 illustrate the different criteria - their respective means as spheres, the standard deviations as squares, the data for the 17 shale plays as small triangles and finally the Barnett data point as the large triangles.

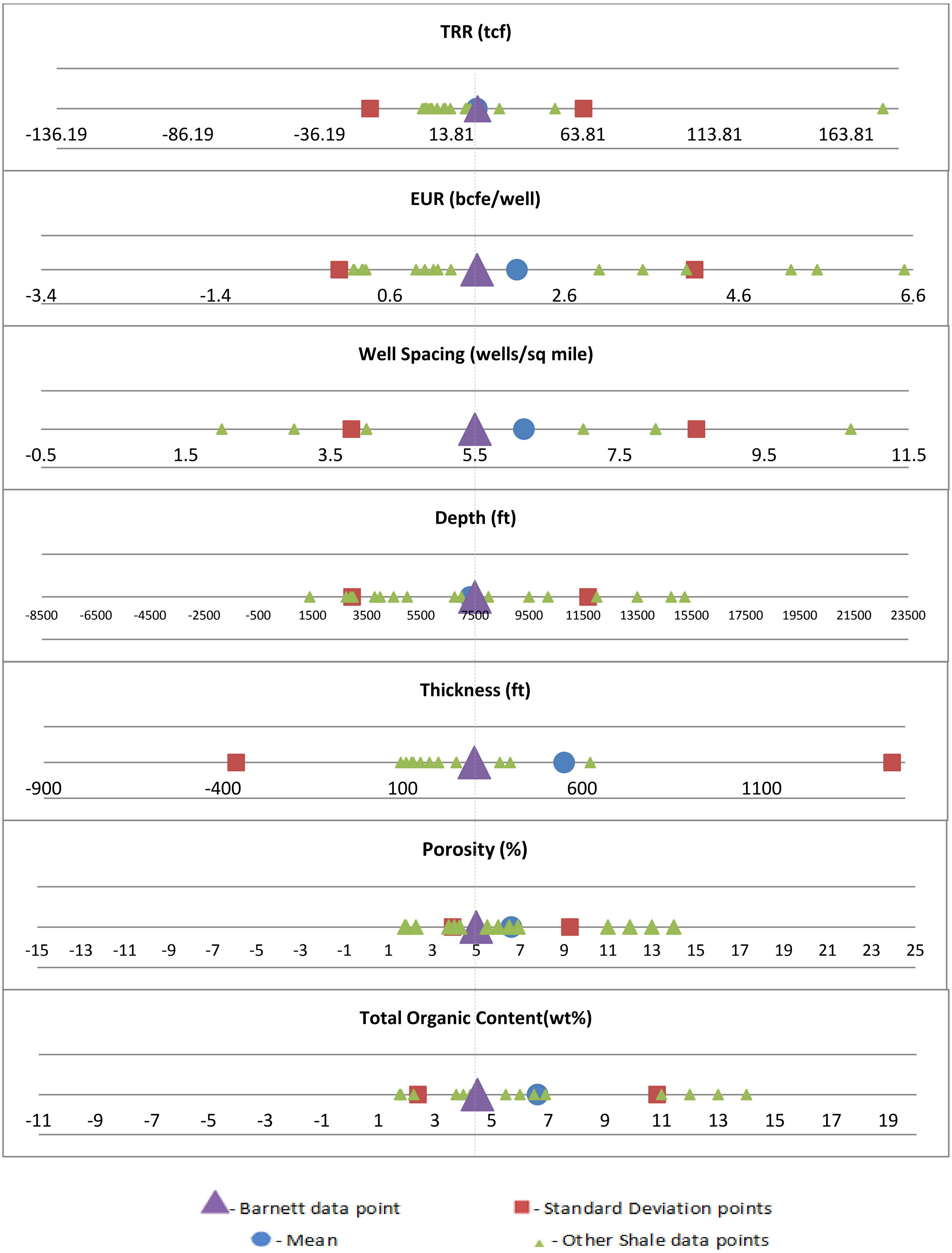

Figure 5.2 – Plots of the properties associated with the 18 US shale plays. This particular layout of results illustrates where the properties of the Barnett shale lie with respect to the means, unit standard deviations and data points of other shale plays.

As the name suggests, Technically Recoverable Resources (TRR) is the fraction of the total resource base measured in trillion cubic feet, which can be extracted using current technology. The Barnett shale represents the third highest TRR in the US next to only Marcellus and Haynesville. The TRR is often mistaken as the EUR - Estimated Ultimate Recovery which is measured in billion cubic feet estimates per well. It is the sum of the proven reserves at a specified time and the cumulative production up to that time (Morehouse 1997). To achieve high productivity rates, understanding well spacing is crucial and can be different for unrelated fields. The depth of US shale regions ranges between 3000ft (900m) to almost 15000ft (4.5km), and yet the average depth of the Barnett field seems to be very close to the mean of all depths. Another interesting criteria is the total organic carbon (TOC) content, which is essentially the total amount of organic matter in a given sample rock.

Plotting the normal distribution in lines next to each other, aids in understanding how the Barnett compares to all the other shale formations in the US. In every case, the Barnett data point is within one standard deviation of the mean. Table 5.3 shows the differences between the means and the average Barnett values. As with most data distributions, there were a few outliers in the case of EUR and TRR – which was usually the Marcellus data as it is significantly larger than most shale plays in the US. Hence, the Barnett proves to be a good case study to be considered for PHAST modelling

	Mean	**Barnett**	**% Difference**
EUR (bcfe/well)	2.06	1.6	28.8%
TRR (tcf)	23.57	23.81	-1%
Well spacing (wells/sq mile)	6.18	5.5	12.4%
Depth (ft)	7322	7500	-2.4%
Thickness (ft)	550.2	300	83.4%
Porosity (%)	6.60	5	32%
TOC (wt%)	6.48	4.5	44%

Table 5.3 – Comparison of the Barnett averages and the means (of all the shale plays in consideration).

Note: Some percentage differences might seem large, but they are still between the standard deviation points. Refer back to Fig. 5.2 as it represents average characteristics for shale reserves.

5.2 Barnett PHAST inputs

A full scale model of a Barnett shale block was modelled on PHAST with an area of 1km^2 and total depth of 2400m (U.S. Energy Information Administration 2011). Using the average values for the properties associated with Barnett, the thickness of the shale layer was modelled to be around 91 metres. From the figure below, it is clear that the geometry of the geological layers wasn't a priority in this investigation. The shale layer is covered by a general sandstone layer (green). Then there is a layer of clay at around 2000m below the surface. Another layer of sandstone continues for approximately 600 metres when it comes across an impermeable rock layer at around 1000m below the surface. Following another section of sandstone, the top 200m has been modelled as gravel. Now might be good time to reiterate the fact that all shale formations are different. These layers would probably not affect the results gathered from the investigation, but modelling those shows capabilities of PHAST if it has to be adapted at any point. Another distinguishing feature in this case study was the presence of five fractures separated by about 12 metres from each other. The fracture gradient was assumed to be 2400m and the porosity of the shale was changed from

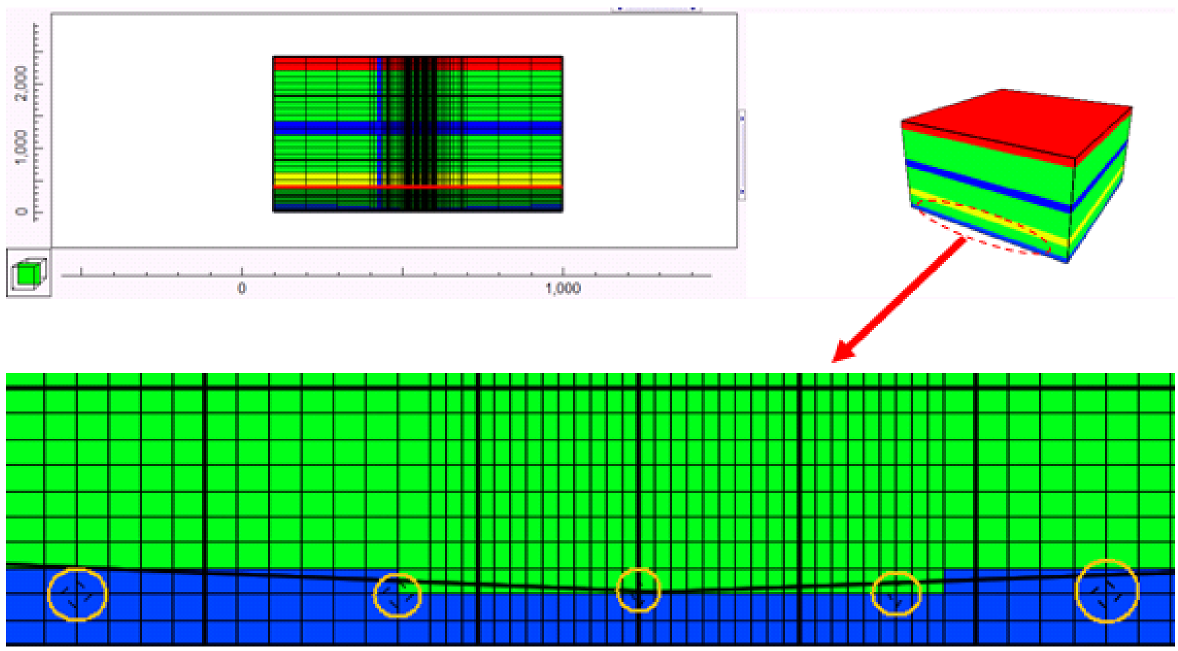

Figure 5.4 – Plane and 3D views of the Barnett case modelled in PHAST (top). Zoomed in view of where the fractures are located in the bottom shale region (bottom). Note the differences in the grid sizes below (discussed later in section 7)

8 to 5%. Figure 5.4 shows a 3D and an X-Y plane view of the modelled Barnett case, along with a zoomed in view of the positions of the fractures.

6. BARNETT STUDY RESULTS

The initial two runs – one for an hour long and one for a day long pressured duration, resulted in negative average flow rates (see Appendix C) near all five fractures. In order to get rid of the issue surrounding negative flow rate values, the print (output) frequencies were adjusted. If the frequencies are set to one time unit instead of two, then PHAST will calculate the results either right before or right after the pressure is dropped to zero. Along with this modification the hydraulic conductivity of the shale was also changed. The new value was the lower extreme of the usual range for shale rocks. In addition, the shale layer was lifted slightly higher than before making sure that this time it covered all of the fractures.

Table 6.1 below shows the results in their mass units over the specified time period. The new values imply that the output frequency modification worked. PHAST now doesn't have enough time to consider all the negative flow back into the fracture. The values are also fairly modest. Realistically the fracture might be at pressure for at most an hour and this

	1 hour		1 day	
Fracture number	**Mass (kg)**	**Cl Mass (kg)**	**Mass (kg)**	**Cl Mass (kg)**
1	0.089	0.032	1.32	0.467
2	0.089	0.032	1.3	0.459
3	0.072	0.025	1.11	0.394
4	0.072	0.025	1.11	0.393
5	0.089	0.032	1.3	0.46
Total Mass	0.411	0.146	6.14	2.173

Table 6.1 – Interpretation of the simulation output data - from average flow rates into estimates of average mass of fluid and chlorine escaping out of the fractures.

corresponds to about 0.4kg of fluid (almost 0.4 litres as the fluid is not pure water) seeping into the shale. This result is still very small compared to the average amount of fresh water required for a typical horizontal well in the Barnett – ranges between 3 and 3.5 million gallons of water over the course of its lifetime.

Similar to the results from the DEMO runs, PHAST calculated the pore velocity values in the Barnett between adjacent grids for each time step. For this particular investigation, only five time steps were taken into consideration due to the requirement of longer simulation times and extensive memory space for a larger number of time steps. In the DEMO run analysis, the velocity gradient vertically above the fracture was examined. Since there were five fractures in the Barnett model, the flow above a single fracture in consideration would be affected by flows from each of the other four. Figure 5.4 shows how the five fractures are symmetrical about the third one on the X-Y plane. And since the properties of the fractures were constant, it was assumed that the flows from factures 1 and 2 would be the same as the flows from fractures 4 and 5. Therefore the vertical column above fracture 3 was considered for the pore velocity analysis.

Appendix C tabulates the data which shows how the pore velocities vary with time across the different layers. In the space of five hours, the fluid only manages to reach the tenth layer out of the 37 modelled in the Barnett – only about 100 metres. The tables of PHAST model data suggested that it considered any value under 10^{-23} as zero. This assumption by PHAST could be challenged since even velocity values of 10^{-10} m/days could be assumed to be zero in the industry and not necessarily anything under 10^{-23}.

The data collected for the analysis consisted of sets of values from three variables – velocity, time and thickness. Figure 6.2 illustrates two types of representations of the data. The first plot compares the changes in velocity with time over the different layers; whereas the second compares the changes in velocity across the layers over the different time steps.

Plot 6.2(a) implies that between most of the layers the velocity increases exponentially (nb log scale). The shapes of the curves between the different layers shows consistency in the calculations, except for one occasion between layers 3 and 4 for the first time step. This "kink" in the curve is similar to the one observed during the DEMO runs, and is discussed in the next section. The plot also proves that the velocities do not undergo significant scale changes between two adjacent layers. This fact is made clearer with the help of figure 6.2(b)

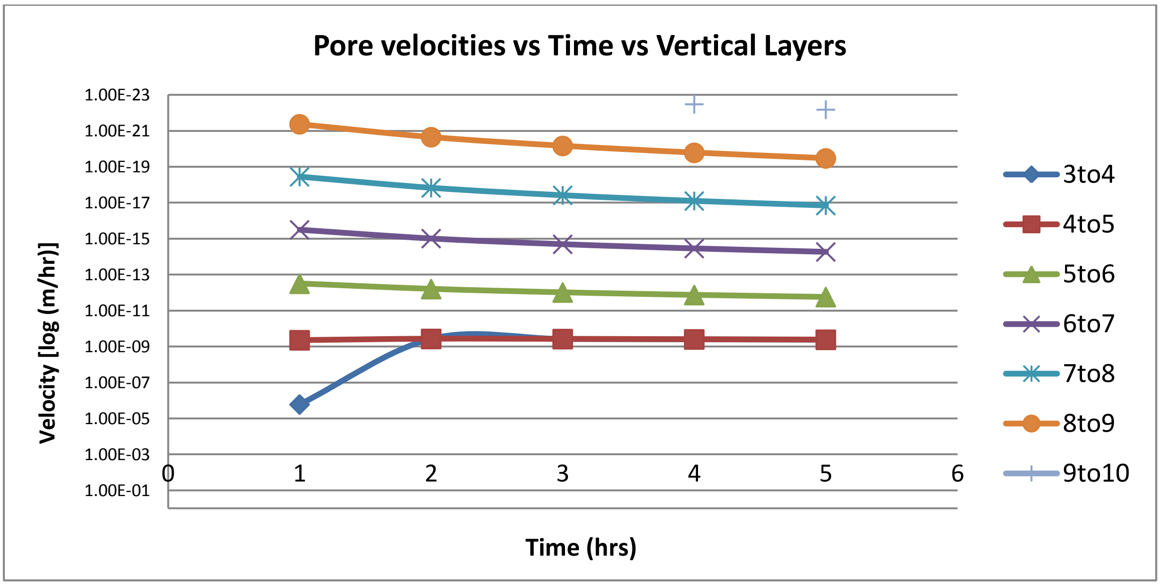

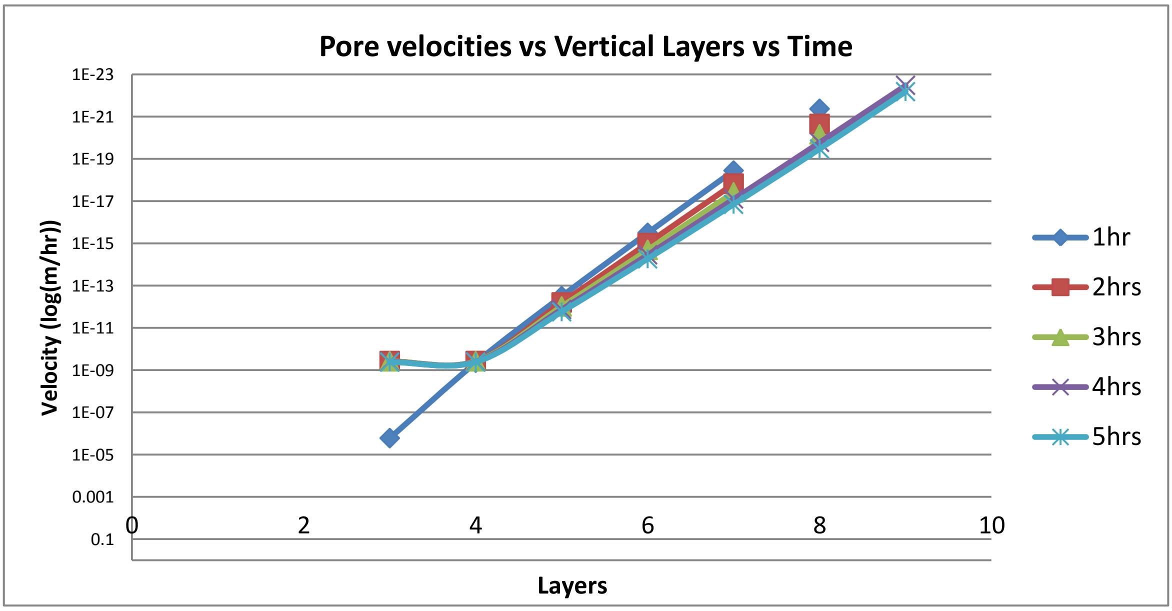

Figure 6.2 (a) and (b) – Curves of pore velocities plotted against time, for seven layer crossovers (a); and plots of the same pore velocities against the layers, for the five time steps (b). The latter graph illustrates how the rate of the velocity changes between the layers does not differ by a large margin over the five time steps (discussed in section 7).

– a different angle in the interpretation of the data. The second figure plots the pore velocities against the layers, and displays how the gradient of the curves are very similar, i.e the rate of change of velocities across the layers for the five time steps.

7. BARNETT STUDY DISCUSSION

Compared to the initial demonstration runs, the Barnett case was modelled to be more applicable to the existing hydraulic fracturing wells. The scenario was also a result of lessons learnt from the DEMO runs. This case was designed to represent 2400 metres of a geology block, and this larger range was expected to give an idea of how far the water could get away with time and how fast it was travelling. The pore velocity results directly above fracture 3 suggested that the values increased exponentially with time across the layers. The shape of the curve across layers 3 and 4 was of particular interest. Figure 6.2(a) showed that there was a significant change in velocities over the first two time steps. PHAST calculated the pore velocity from the grid surrounding the fracture after 1 hour – which was the time at which the pressure within the fracture was released. Hence the corresponding velocity result was high due to the pressure head of 2400m in the fracture. The plot also demonstrates how it did not take the fluid much time to reach a steady state value, as it reached the constant by the second time step (2 hours). This explains why there was an inconsistency – "kink", in the shape of that particular curve.

The results for the average flow rates were used to estimate the mass of the fluid and the chlorine that was transported out of the fractures. One would expect these mass values to be same across all five fractures as they all have the same properties. The potential reasons for this inconsistency were investigated and it was concluded that this happened because of the differences in grid sizes. Figure 5.4 on page 24 illustrates how only fractures 3 and 4 lie in the area with smallest grid sizes which corresponded with their comparatively smaller average flow rates. More accurate and consistent values of flow rates can be achieved if the grid encompassing the fractures could be designed to be as small as possible. This would create millions more grids which would then force PHAST to take hours to simulate the scenario calculating gigabytes of information. If only the flow rate out of the fracture is of interest, then a very simplified alternative would be to just model a single grid small enough to fit the fracture, and not bothering with a large scale geological model.

All the simulations assume chlorine to be the main chemical present in the fluid. This could be adapted to chloride which would be more useful for tracing the flow of the fluid. Simulating chloride would also help in conducting a chloride mass balance – which has been extensively used for estimating aquifer recharge in porous media aquifers (Cook 2003).

The summation of the mass of fluid spreading into the shale shows very low values. Similar to the argument made for the DEMO run results, a lot of the water could be trapped in the lengths of the well during the fracturing procedure. And over the course of a wells' lifetime, using 3 million gallons of water is not unlikely. But 0.4 litres calculated still seems to be an underestimate for the industry values. From all the input parameters and results, it is suspected that the fracture geometry could provide the explanation for the low mass values. An intricate and a more intricate network of cracks stemming from a single fracture could have surface area much higher than $3m^2$ (contrary to the assumptions in the simulations) resulting in much higher mass flow rates. It has been mentioned before that every shale play has different properties from the other – the fracture gradients, porosity, hydraulic conductivity and the specific storage will all influence how the crack forms and how much water would seep out.

On the other hand, the pore velocity results were almost certainly overestimates despite the insignificant scales of their values. The simulations did not consider the actual or close to real chemicals used for hydraulic fracturing. The reactions of these contaminants with the minerals in the geology and their diffusion into the deep groundwater would reduce the size of the calculated velocities. Therefore the average flow rates are more realistic of the two evaluated results obtained from these simulations.

The results acquired from the Barnett case can be considered to be as the average results expected for US shale plays (referring back to figure 5.2 on page 22). Thus the product of an adapted version of such a model could be used to estimate average leakage rates and the velocity profiles through the geological layers.

8. GENERAL DISCUSSION

The results that were considered in this investigation – the average flow rates and the pore velocities, gave indirect indications of how much water could be used to create a fracture and the distances covered by the fluid with time respectively. This data would help engineers and environmental scientists to assess the potential exposure of the fracturing fluid into useable groundwater. And since the hazardous properties of a lot of the chemicals present in this fluid are known – such an investigation could be used as a part of a risk assessment tool for hydraulic fracturing (Risk = Hazard x Exposure).

In real life situations there are other parameters that have to be taken into consideration in order to achieve accurate data. One aspect that has not been addressed in these investigations is the flowback pressure. Once the shale has been fractured for the desired amount of time, the water is pumped back to the surface pulling out the hydrocarbons entailing the flowback water. In this investigation it was assumed that the pressure would drop to zero after the fracturing period, which in reality would allow the fracture to close due to the surrounding pressure gradient. But in practice, this is a negative value which aids in pumping the water out of the fractures. Therefore, a suggested modification to this investigation would be to model negative pressures after certain time steps and see if the results show any significant change. In this study, only the amount of water seepage was recorded. And in theory all of this would be pumped back onto the surface after the procedure. But studies have shown that this is not always the case. Only about 15-80% of the fracturing water is usually recovered from hydraulic fracturing wells.

The fluid does not necessarily have to escape through the shale. Poorly designed completions of wells and weak casing materials could also leak the fracturing fluid. It is important to note that some wells extend to about 2 miles downwards before any fracturing takes place. This could give the fluid plenty of opportunity to escape.

A single well can undergo several occasions where high pressure frac fluid is being pumped down into the fractures. This would also increase the water usage per well – another feature that could be added to the PHAST model by creating cycles of pressure changes, e.g. 2400m at T=1, -2400m at T=2, 0 at T=3 and back to 2400m at T=4, and so on.

PHREEQC (segment of PHAST) allows the chemistry file to be moulded to the preferences of the user. This input file could potentially be adapted to incorporate acids (such as hydrochloric acid – very common in frac fluids) and other dangerous compounds such as ethylene glycol. These chemicals can then be traced using the outputs from PHAST – which is crucial in estimating the reach of harmful contaminants outside the fractures in shale. A monitoring well could be considered in the actual field and this feature can be included in the boundary conditions of the modelling software.

Once all the known parameters have been included in the model, its effectiveness and accuracy in the industry could then be tested by comparing the simulation results of the water usage to the actual quantities of fluid used by the well. Applying this test to several existing shale plays will give an indication of how useful this tool could be in the industry, and based on its merits this free tool could then be used to predict water usage for potential shale field developments.

As discussed earlier, the boundary conditions in PHAST could be set to make the fracture act either like a leaky boundary, specific head (used in this project), an underground river or even a reverse well. It is unknown how exactly these fractures might behave 2km underground and hence more research in this field will help in justifying the most appropriate boundary condition. One limitation that the modelling software seems to exhibit is the requirement of potentially gigabytes of data space and hours of simulation periods if more complex data is modelled. This could be overcome by perhaps sub-dividing the model into smaller segments to be simulated separately or just waiting for more efficient versions of it to be released.

For this particular project, there were several options for the next stage of the investigation. The Barnett simulation could have been run over longer time periods – up to 100 days instead of 5, chlorine could have been replaced by hydrochloric acid, and of course the flow back pressures could have also been modelled. Model Viewer is an extension for PHAST and MODFLOW which helps in visualizing both scalar and vector outputs from the simulations. In the long run this would save time going through pages of text files trying to understand the data. For example Model Viewer can be made to display the concentration profiles of a particular contaminant as in figure 8.1 – which shows the top view of Mg concentrations for a PHAST tutorial example.

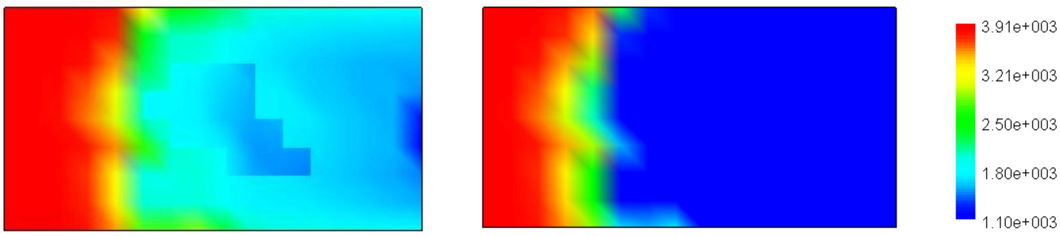

2000 years **4000 years**

Figure 8.1 – Top views of changes in concentration maps of Magnesium over 2000 and 4000 years - illustrated using a PHAST example file.

9. CONCLUSION

The primary objective of this investigation was to assess the water leakage from fractures by creating a modelling toolkit which could be a segment of a larger risk assessment process. This simulator was expected to produce estimates of the volumes of water and distances that it would be able to cover. The end product of the investigation that was carried out was a FORTRAN based tool – PHAST, moulded to represent hydraulic fracturing scenarios in the most reasonable ways. In most cases the results that were obtained from the models corresponded to the initial hypothesis and expectations. Assuming that there are no problems establishing the well, the models implied that the fluid leakage into the shale should be very small and can be comparable to industry values if the volumes in the length of the pipe are considered. The analysis on the pore velocities showed how insignificant the values could be in the conceptual model. The values achieved are expected to be even lower if the geochemical reactions and the flowback pressure were also to be considered. And hence, the conceptual models in this investigation gave overestimates of the leakage volumes. This tool will be valuable in the risk assessment of shale plays under appraisal as the results will help engineers in evaluating the potential threats to the water resources. Not only did this project produce a potential screening toolkit but it also assisted in learning the concepts behind geological formations, hydrocarbon extraction and the environmental risks associated with drilling techniques. The demand for gas will keep growing and hydraulic fracturing will play an important role in its production. Therefore it is crucial that the methods prioritize environmental safety above anything else and hopefully the outcome of this project will in some way contribute to this movement.

10. BIBLIOGRAPHY

Arthur, A.J.D. et al., 2008. Hydraulic Fracturing Considerations for Natural Gas Wells of the Marcellus Shale.

Cook, P.G., 2003. A guide to regional groundwater flow in fractured rock aquifers.

Daneshy, A., 2010. Hydraulic Fracturing To Improve Production. *Tech 101*, 6, pp.14-17.

Fisher, M.K. et al., 2004. SPE 90051 Optimizing Horizontal Completion Techniques in the Barnett Shale Using Microseismic Fracture Mapping. *Society of Petroleum Engineers*.

Foda, A. et al., 2011. Natural Gas Extraction Using Hydraulic Fracturing: Creating a Sustainable Path Forwards. , 15222(412).

Halliburton, 2008. U . S . Shale Gas: An unconventional Resource. Unconventional Challenges.

LaFollette, R., 2010. Key Considerations for Hydraulic Fracturing of Gas Shales.

Morehouse, D.F., 1997. The Intricate Puzzle of Oil and Gas “ Reserves Growth .” *EIA*, (July).

Ramudo, A. & Murphy, S., 2010. Hydraulic Fracturing – Effects on Water Quality. *Cornell University*.

TPG, 2011. A Decade of Drilling. , (August).

U.S. EPA, 2011. Considerations for Fate and Transport Evaluation Of Potential Release Scenarios during Hydraulic Fracturing Operations.

U.S. Energy Information Administration, 2011. Review of Emerging Resources: U.S. Shale Gas and Shale Oil Plays. , (July).

U.S. Environmental Protection Agency, 2010. Hydraulic fracturing research study. *EPA/600/F-10/002*, pp.1-2.

Waters, G. et al., 2009. Utilization of Real Time Microseismic Monitoring and Hydraulic Fracture Diversion Technology in the Completion of Barnett Shale Horizontal Wells. *Society of Petroleum Engineers*, (Proceedings of Offshore Technology Conference), pp.1-11.

11. ACKNOWLEDGEMENTS

I owe sincere and earnest thankfulness to:

Dr G.T. Parker

Dr Richard Keck, BP plc.

Ms Natalyn Ala, Atkins

U.S. Geological Survey - PHAST, ModelMuse and Model Viewer

12. APPENDICES

Risk Assessment Retrospective

There were no hazards or risks associated during the entire project as stated initially at the start of the year. There was no practical work involved – which eliminated any occurrences of risks.

Appendix A - Inputs

	Shale	**Clay**	**Sandstone**	**Limestone**
Hydraulic conductivity k_x (m/s)	10E-11	10E-10	5E-8	1E-8
Porosity (%)	8	40	32	25
Specific storage (ft^{-1})	10E-6	2E-4	10E-6	10E-6

Figure 12.1 – Inputs of three of the important properties used in the DEMO runs. Note: All the data are average values.

Courtesy of AQTESOLV. Available at http://www.aqtesolv.com/aquifer-tests/aquifer_properties.htm

Appendix B – U.S. Shale comparisons

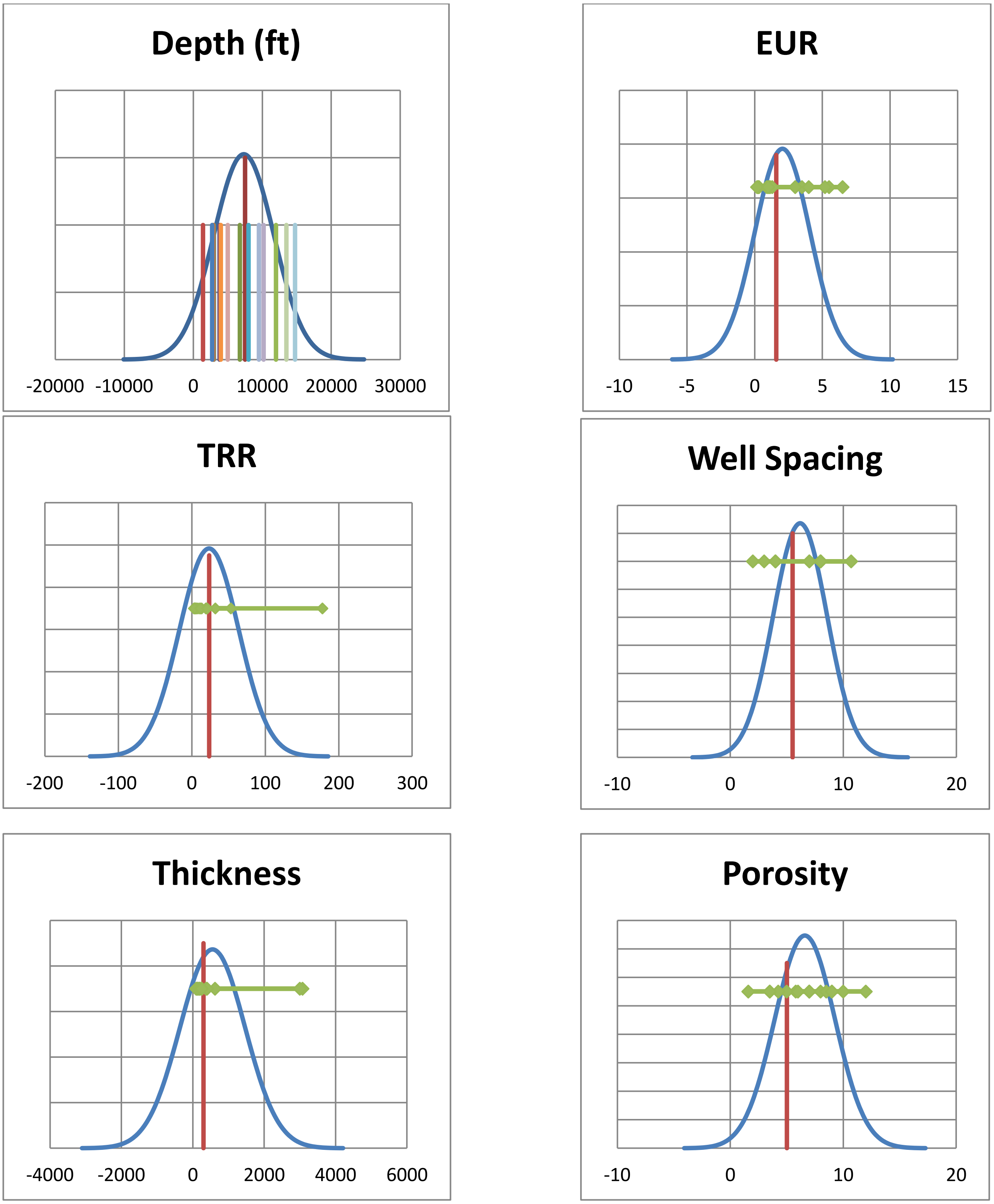

Figure 12.2 – Initial approach in comparing Barnett properties to the other shales in the form of normal distribution bell curves. Red line signifies the position of the Barnett with respect to the curve.

APPENDIX C – Results

Below are the tables of the simulation average flow rate data that were plotted and discussed in this document extracted directly from the spreadsheets.

	Case 1							
	2400m		6000m					
	1hr		1min		1hr		1day	
T.Step	Flow	Cl	Flow	Cl	Flow	Cl	Flow	Cl
1	1.70E-08	9.12E-06	7.07E-10	9.12E-06	4.24E-08	9.12E-06	1.02E-06	9.12E-06
kg/s	4.72E-12	2.53E-09	1.18E-11	1.52E-07	1.18E-11	2.53E-09	1.17905E-11	1.056E-10

Case 2							
2400m		6000m					
1hr		1min		1hr		1day	
Flow	Cl	Flow	Cl	Flow	Cl	Flow	Cl
8.11E-08	4.56E-06	3.38E-09	4.56E-06	-2.03E-07	4.63E-06	4.87E-06	6.29E-06
2.25E-11	1.27E-09	5.63E-11	7.60E-08	-5.63E-11	1.29E-09	5.63E-11	7.28E-11

Case 3							
2400m		6000m					
1hr		1min		1hr		1day	
Flow	Cl	Flow	Cl	Flow	Cl	Flow	Cl
-4.69E+03	-1.66E+03	-1.17E+04	-4.16E+03	1.17E+04	-4.16E+03	-9.50E+04	-3.37E+04
-1.30E+00	-4.62E-01	-1.95E+02	-6.93E+01	3.26E+00	-1.15E+00	-1.10E+00	-3.90E-01

Case 4							
2400m		6000m					
1hr		1min		1hr		1day	
Flow	Cl	Flow	Cl	Flow	Cl	Flow	Cl
-1.76E+04	-6.23E+03	-2.35E+04	-8.35E+03	-4.40E+04	-1.56E+04	-2.11E+05	-7.50E+04
-4.88E+00	-1.73E+00	-3.92E+02	-1.39E+02	-1.22E+01	-4.33E+00	-2.45E+00	-8.68E-01

Case 5							
2400m		6000m					
1hr		1min		1hr		1day	
Flow	Cl	Flow	Cl	Flow	Cl	Flow	Cl
-9.44E+05	-3.35E+05	-2.36E+06	8.35E+05	-2.36E+06	-8.37E+05	-2.85E+06	-1.01E+06
-2.62E+02	-9.29E+01	-3.93E+04	1.39E+04	-6.55E+02	-2.32E+02	-3.30E+01	-1.17E+01

Case 6							
2400m		6000m					
1hr		1min		1hr		1day	
Flow	Cl	Flow	Cl	Flow	Cl	Flow	Cl
4.49E-04	2.36E-04	1.34E-06	7.46E-05	8.06E-05	1.06E-04	1.93E-03	7.63E-04
1.25E-07	6.56E-08	2.23E-08	1.24E-06	2.24E-08	2.94E-08	2.23E-08	8.83E-09

The next few tables are the flow rate results obtained from the Barnett simulation:

	Barnett	*1*	*2400m*	*First run*						
	1hr									
	Flow					*Cl*				
	1	*2*	*3*	*4*	*5*	*1*	*2*	*3*	*4*	*5*
1	*-1172*	*-1496*	*-1004*	*-1013*	*-1172*	*-415.5*	*-530.3*	*-356*	*-359.3*	*-415.5*
kg/s	*- 0.32555556*	*- 0.4155556*	*- 0.2788889*	*- 0.281389*	*- 0.32555556*	*- 0.1154167*	*- 0.147305556*	*- 0.0988889*	*- 0.0998056*	*- 0.1154167*

	First Run								
1 day									
Flow					*Cl*				
1	*2*	*3*	*4*	*5*	*1*	*2*	*3*	*4*	*5*
-1185	*-6332*	*-8219*	*-9090*	*-1185*	*-420.2*	*-2245*	*-2914*	*-3223*	*-420.2*
-0.0137153	*-0.073287*	*- 0.09512731*	*-0.1052083*	*-0.0137153*	*-0.0048634*	*-0.0259838*	*-0.0337269*	*-0.0373032*	*-0.0048634*

	Barnett	2	*Second run: Modification – Time steps were halved*							
	1hr									
	Flow					Cl				
	1	2	3	4	5	1	2	3	4	5
	8.96E-02	8.93E-02	7.18E-02	7.17E-02	8.94E-02	3.18E-02	3.17E-02	2.54E-02	2.54E-02	3.17E-02
kg/s	2.49E-05	2.48E-05	1.99E-05	1.99E-05	2.48E-05	8.82E-06	8.79E-06	7.07E-06	7.07E-06	8.80E-06

1 day									
Flow					Cl				
1	2	3	4	5	1	2	3	4	5
1.32E+00	1.30E+00	1.11E+00	1.11E+00	1.30E+00	4.67E-01	4.59E-01	3.94E-01	3.93E-01	4.60E-01
1.52E-05	1.50E-05	1.29E-05	1.28E-05	1.50E-05	5.40E-06	5.31E-06	4.56E-06	4.55E-06	5.32E-06

Next few tables contain the pore velocity values between grids investigate in the document:

1 day							
	Case 3						
	2	4	8	12	16	20	24
3 to 4	1.75E-01	1.30E-07	1.38E-07	1.41E-07	1.44E-07	1.44E-07	1.44E-07
8 to 9		5.60E-19	5.40E-18	2.20E-17	6.00E-17	1.36E-16	2.81E-14
1 day							
	Case 4						
	2	4	8	12	16	20	24
3 to 4	1.04E+00	4.52E-07	1.36E-07	9.41E-08	8.86E-08	8.74E-08	8.67E-08
8 to 9	2.79E-16	1.38E-15	7.27E-15	1.93E-14	3.92E-14	6.89E-14	1.10E-13

1hr					
	Barnett				
Fracture 3	1	2	3	4	5
9to10	0	0	0	3.28E-23	6.56E-23
8to9	4.27E-22	2.23E-21	6.86E-21	1.65E-20	3.38E-20
7to8	3.59E-19	1.49E-18	3.84E-18	7.92E-18	1.42E-17
6to7	3.18E-16	9.77E-16	2.03E-15	3.49E-15	5.41E-15
5to6	3.18E-13	6.28E-13	9.72E-13	1.35E-12	1.75E-12
4to5	4.42E-10	3.74E-10	3.81E-10	3.98E-10	4.16E-10
3to4	1.66E-06	3.74E-10	3.82E-10	3.99E-10	4.18E-10

Appendix D – Hydraulic fracturing fluids

Additive Type	Main Compound	Purpose
Diluted acid (15%)	Hydrochloric acid *	Dissolve mineral/sand initiates cracks in rock
Biocide	Glutaraldehyde	Bacterial control
Corrosion inhibitor	N,n-dimethylformamide	Prevents corrosion
Breaker	Ammonium persulfate	Delays breakdown of gel polymers
Crosslinker	Borate salts	Maintains fluid viscosity at high temperature
Friction reducers	Polyacrylamide *	Minimize friction between the fluid and the pipe
	Potassium chloride	
	Mineral oil	
Gel	Guar gum or Hydroxyethylcellulose *	Thickens water to suspend the sand
Iron Control	Citric Acid	Prevent precipitation of metal oxides
Oxygen scavenger	Ammonium bisulfite **	Remove oxygen from fluid to reduce pipe corrosion
pH adjusters	Potassium or sodium carbonate	Maintains effectiveness of other compounds (e.g. crosslinker)
Proppant	Silica quartz sand	Keeps fractures open
Scale inhibitor	Ethylene glycol	Reduced deposition on pipe
Surfactant	Isopropanol	Increase viscosity of fluid
* indicates degree of health hazard in concentrated form		

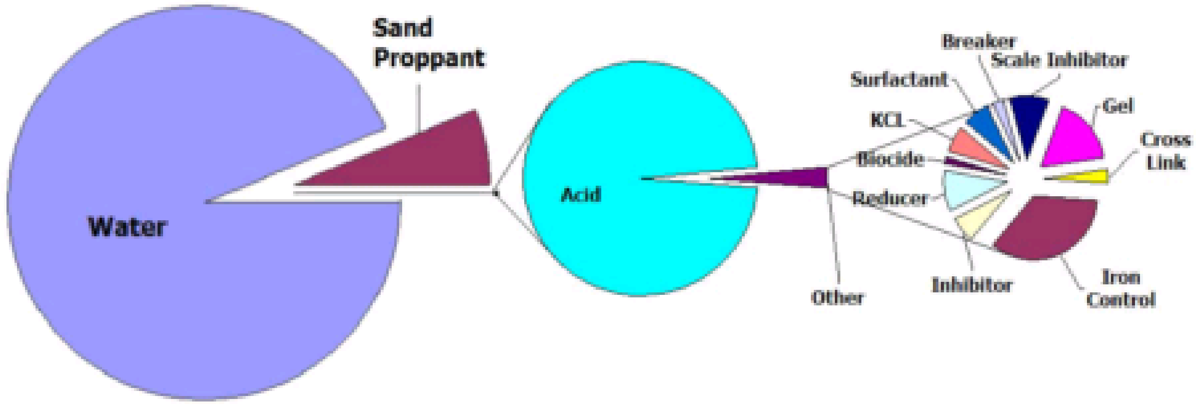

Figure 12.4 – Breakdown of a typical hydraulic fracturing fluid featuring few of the numerous chemicals (Ramudo & Murphy 2010) – *(top). Illustration of the breakdown frac fluid used in the Marcellus shale play* (Arthur et al. 2008) – *(bottom).*

Figure 12.4 – Average property data collected on 18 US shale plays (U.S. Energy Information Administration, 2011). Calculated means and standard deviations written at the bottom of the figure.

	Shale Formation	EUR (Bcfe/well)		TRR (Tcf)		Well Spacing (wells/sq. mile)		Depth (ft)	Thickness (ft)	Porosity (%)	Total Organic content (%wt)	Area (sq. miles)	
		Active	*Undeveloped*	*Active*	*Undeveloped*	*Active*	*Undeveloped*					*Active*	*Undeveloped*
Northeast	Marcellus	3.5	1.15	177.9	232.44	8	8	6750	125	8	12	10622	84271
	Devonian Big Sandy	0.325	0.325	6.47	0.92	8	8	3800	175	10	3.75	8675	1994
	Devonian Low Thermal Maturity	0.2942		13.53		7		3000	371	7			
	Devonian Greater Siltstone	0.193		8.46		10.7		2911	623	5.8			
	New Albany	1.1	~	10.95	~	8	~	2750	200	12	13	1600	41900
	Antrim	0.28		19.93		7		1400	95	9	11	12000	
Gulf Coast	Haynesville	6.5	1.5	53.3	19.41	8	8	12000	250	8.5	2.25	3574	5426
	Eagle Ford (Dry Gas)	5.5		4.38		4		7000	200	9	4.25	200	~
	Floyd-Neal/Conasauga	0.9		4.37		2		8000	130	1.6	1.8	2429	
Mid-Continent	Fayetteville	1.15	2.25	4.64	27.32	8	8	4000	110	5	6.9	9000	
	Woodford (Western)	4		19.26		4		9500	150	7	6.5	2900	
	Woodford (Central)	1		2.95		4		5000	250	6	4	1800	
	Cana Woodford	5.2		5.72		4		13500	200	7	6	688	
Southwest	**Barnett**	**1.6**	**1.2**	**23.81**	**19.56**	**5.5**	**8**	**7500**	**300**	**5**	**4.5**	**4075**	**2383**
	Barnett-Woodford	3		32.15		4		10200	400	~~	5.5	2691	
Rocky Mountain	Hilliard-Baxter-Mancos	0.18		3.77		8		14750	3075	4.25	1.75	16416	
	Lewis	1.3		11.63		3		4500	250	3.5		7506	
	Mancos	1		21.02		8		15250	3000	3.5	14		
	Mean	2.056		23.57		6.12		7322.8	550.2	6.60	6.48	5611.7	
	Standard deviation	2.04		40.56		2.39		4358.5	913.8	2.67	4.1	4809.06	